

## SOFT-IMPACTING MICROMECHANICAL RESOSWITCH ZERO-QUIESCENT POWER AM RECEIVER

Ruonan Liu, Jalal Naghsh Nilchi, Wei-Chang Li, and Clark T.-C. Nguyen  
University of California at Berkeley, Berkeley, California, USA

### ABSTRACT

A micromechanical resonant switch-based envelope detector employing a soft-impact cantilever output electrode to affect a linear input amplitude-to-output level gain has successfully received, filtered, amplified, and demodulated an input AM signal over a 63-kHz carrier, effectively demonstrating a zero-quiescent power AM receiver to complement a previous such FSK receiver [1]. The RF front-end achieves a power gain of 30dB and demodulates without needing a power hungry local oscillator. Key to operation as an AM receiver is the linear analog amplification (as opposed to binary amplification of [1]) enabled by the flexible soft-impact output electrode. The higher  $Q$  of 1200 of the polysilicon device with Ru-silicide contact further increases the receiver sensitivity to  $-68\text{dBm}$ , which is 8dB better than that of [1]. The ability of this device to AM demodulate while consuming zero power during standby periods makes it ideal for use in ultra-low power long-distance receiver applications, such as the clocks that wirelessly receive atomic clock time over thousands of miles via AM over a 60-kHz carrier [2].

### INTRODUCTION

Low frequency (LF) wireless communication from 30-300 kHz has the unique ability to transfer information over thousands of miles [2]. Radio clocks that acquire atomic time from centralized locations (e.g., from NIST in the U.S. via AM at 60 kHz using the WWVB standard [2]) are perhaps the most recognizable consumer applications in this frequency range, but there are other less known, but important, positioning and communication applications. Thanks to the long-range nature of LF signals, a single base station can broadcast over the entire U.S.

If LF receivers could occupy single chips and consume zero power while actively listening for incoming information, then this frequency band might also be useful for updating of consumer products, e.g., firmware updates that do not require interconnect connection. This would make for a compelling application for the all-mechanical zero-quiescent power OOK receiver front-end of [1] that utilized micromechanical resonant switches (resoswitches) to demodulate FSK signals.

Smaller size and zero-quiescent power consumption would also be beneficial for the aforementioned time transfer applications. For these, however, the WWVB standard calls for AM modulation, rather than OOK, or even FSK. Like their aperiodic mechanical switch brethren used for RF switching [3] and more recently for digital logic [4], the resoswitches used in [1] have abrupt on/off transitions—something very useful for their prescribed applications, but not so useful for AM demodulation, which requires a more gradual transition from “off” to “on”, preferably a linear gain profile, as illustrated in Figure 1.

Pursuant to enabling AM detection and demodulation

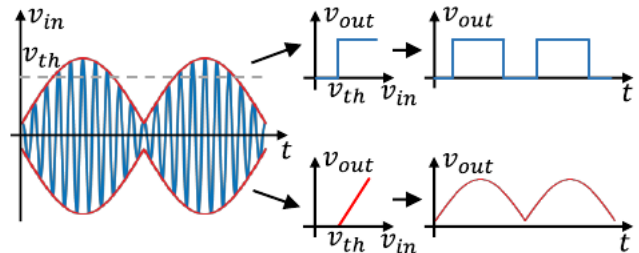


Figure 1: (Top): Abrupt on/off transition removes AM information. (Bottom): Gradual gain characteristic preserves the AM signal envelop, allowing AM demodulation.

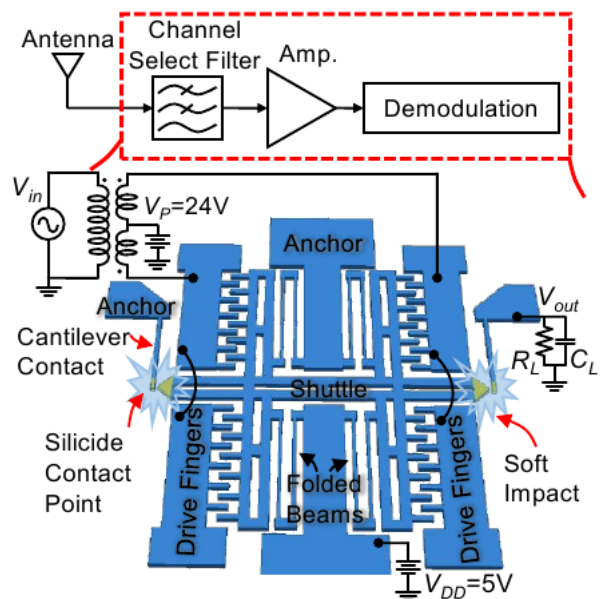


Figure 2: Schematic summary illustrating the AM receiver functionality of the soft-contact resoswitch device. Here, following the antenna, the resoswitch with silicided soft-electrode contact filters out interferers and envelop-detects the input AM modulated signal in one device.

at LF, this work presents a resoswitch design that employs a soft impact electrode to provide a linear gain profile. This, in addition to its inherent resonance-enabled frequency selectivity, allows the device to select a desired 63-kHz AM carrier, provide power gain, and envelop-detect (demodulate) the signal, all while consuming zero quiescent power.

### AM RECEIVER STRUCTURE AND OPERATION

Figure 2 summarizes the structure and operation of the all-mechanical AM receiver. Here, an antenna receives the information-rich AM signal in the desired channel alongside unwanted interferers in adjacent channels and directs the combined signal to the resoswitch input. As shown, the resoswitch comprises a folded-beam comb-driven resonant structure, much like conventional renditions [5], except this

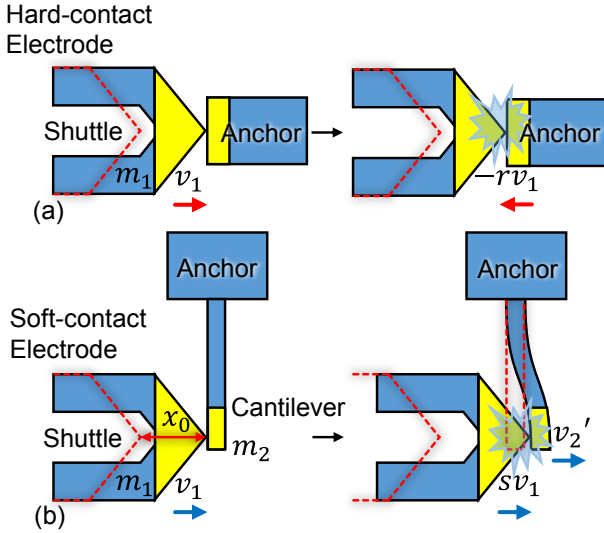


Figure 3: Illustrations describing the contact dynamics of soft and hard contact electrodes. The hard-contact electrode (a) reverses the shuttle direction, while the soft-contact electrode (b) merely yields to the shuttle.

one can impact the identified switch contact points when its resonance vibration amplitude exceeds a certain threshold. Each impact connects the switch terminals to the supply voltage  $V_{DD}$ , allowing current to flow from the supply to the terminals, thereby delivering power to them, i.e., providing power gain.

As Figure 2 indicates, the all-mechanical resoswitch device performs all functions normally needed for AM reception, including filtering, amplification, and demodulation. It filters mechanically via its bandpass biquad voltage-to-velocity frequency response, which is conveniently thin and sharp enough to select the desired 52 Hz channel while suppressing out-of-channel interferers. Removal of interferers of course prevents them from generating intermodulation components through subsequent nonlinearity, which then allows the following stages to be quite nonlinear. More to the point, it allows use of a very nonlinear switching amplifier, such as realized via the resonant impact switch depicted in Figure 2.

Resonant impacting also enables demodulation, the type of which, i.e., OOK, FSK, or AM, depends upon the hardness of the contact.

### Hard Versus Soft Contact

Figure 3(a) and (b) respectively illustrate the differences between the hard contact of previous work [1] realized using an output switch electrode firmly clamped to the substrate; and the soft contact of this work, realized by a cantilever structure that bends when experiencing an impact. In each case, the impact electrode sits  $x_0$  away from the tip of the shuttle at rest.

The hard and soft contact cases differ in the slopes of their input-amplitude versus output voltage curves, where the former's is quite large, to the point of realizing a practically instantaneous on/off transition; and the latter's much smaller, allowing for a slower transition that enables AM demodulation.

The reason for the difference between the two lies in the contact force, which takes the form

$$F_c = \frac{m_1(v_1' - v_1)}{t_c} \quad (1)$$

where  $m_1$  is the shuttle mass,  $t_c$  is the contact time, and  $v_1$  and  $v_1'$  are the pre- and post-impact velocities, respectively, of the shuttle. In the hard-contact scenario of Figure 3(a), the electrode remains stationary during impact and the shuttle recoils after impact at

$$v_1' = -rv_1 \quad (2)$$

where  $r$  ( $0 < r < 1$ ) is a coefficient that accounts for the energy loss due to impact, governed mostly by properties of the contact material, e.g., hardness, roughness, etc.

On the other hand, when the contact electrode is a compliant cantilever, as in Figure 3(b), the impact does not reverse the direction of the shuttle's velocity, and

$$v_1' = sv_1 \quad (3)$$

where  $s$  ( $0 < s < 1$ ) is determined by contact dynamics governed largely by the mechanical impedance of the cantilever, especially if its stiffness  $k_2$  is much smaller than the contact stiffness due to material hardness. The output voltage derives from a resistive divider

$$v_{out} = \frac{R_L}{R_{on} + R_L} V_{DD} \quad (4)$$

where

$$R_{on} \approx R_o - \phi F_c \quad (5)$$

where  $R_o$  is a low contact force initial resistance, and  $\phi$  models the dependence of contact resistance  $R_{on}$  on contact force [6]. Combination of (1) to (5) then yields

$$v_{out} \approx \begin{cases} \frac{m_1 \phi V_{DD}}{t_c R_L} (1+r)v_1 & (\text{hard contact}) \\ \frac{m_1 \phi V_{DD}}{t_c R_L} (1-s)v_1 & (\text{soft contact}) \end{cases} \quad (6)$$

Since the pre-impact closing velocity  $v_1$  increases with input amplitude, (6) confirms that the input-amplitude to output voltage transfer function has a much smaller slope for a soft contact than a hard contact, allowing the former to affect AM demodulation.

### Soft-Contact Enabled Squegging Suppression

Another benefit of soft-contact electrodes lies in the suppression of squegging [9], in which impact-derived disturbances to the natural resonance induce fluctuations in resonator displacement amplitude and phase. For more insight, Figure 4 plots simulated displacement over time for several hard-contact and soft-contact scenarios. In each plot,  $x_1$  and  $x_2$  represent displacements of the resonator and the contact electrode, respectively, as labelled in Figure 3.

In Figure 4(a), a small  $F_{drive}$  at frequency  $f_1$  drives the shuttle into resonance. Before impact,  $x_1$  is  $90^\circ$  phase-shifted from  $F_{drive}$ . When  $x_1$  exceeds  $x_0$ , the shuttle makes contact with the (hard) electrode. Each contact induces an abrupt change in the phase of  $x_1$  that renders the resonator out of sync with  $F_{drive}$ . This reduces drive efficiency, causing the amplitude of  $x_1$  to decrease, resulting in missed shuttle impacts, as shown. No longer impacting, the phase-shift corrects, the resonator ‘‘catches up’’ to again lag  $90^\circ$

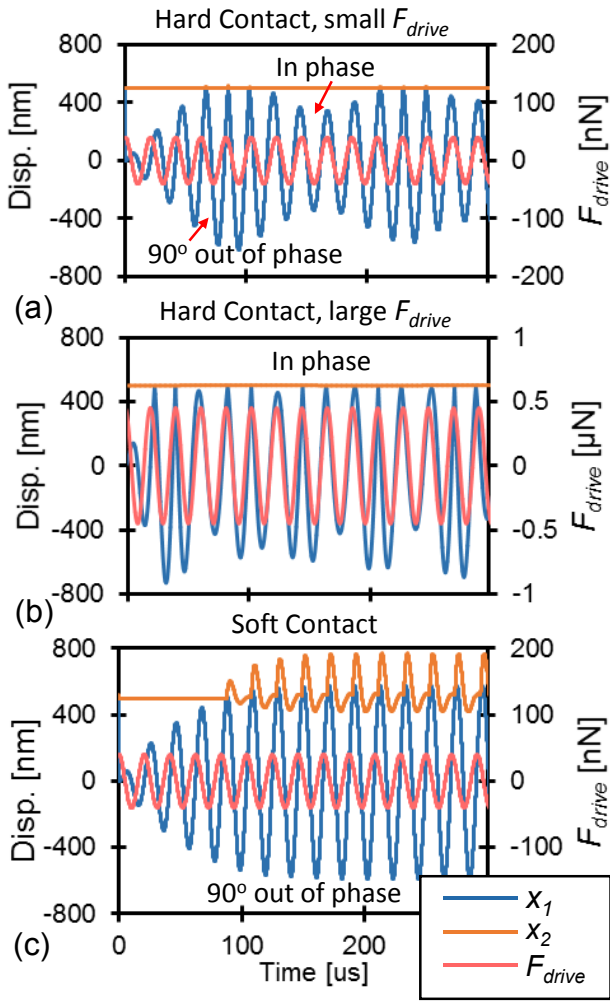


Figure 4: Simulation of transient dynamics of (a) hard-contact with small input force; (b) hard-contact with large input force; and (c) soft-contact.

from the drive force, raising the drive efficiency and allowing the displacement amplitude to again increase.

The dynamics depend highly on energy loss mechanisms at impact, which are difficult to model and predict. The resonator often exhibits chaotic behavior [7], where the output voltage is quite unstable. Since there are still impacts, the output capacitive load still charges, but now much more slowly than if the shuttle impacted on every cycle. As a result, the receiver still works, just slower than ideal, i.e., with degraded bit rate.

For the case of a hard contact, restoring a high bit rate calls for more input energy to overcome the described dephasing energy losses, as shown in Figure 4(b), where a much larger input force amplitude compels the shuttle to displace in phase with the drive force, thereby raising the drive efficiency and allowing impact on each cycle. By raising the needed input energy for a high data rate, squegging essentially compromises the sensitivity of a receiver employing a hard-contact resoswitch.

A soft-contact electrode, on the other hand, allows the shuttle velocity to slowly dissipate instead of directly bouncing back and hence reduces the change in phase on each contact, thereby suppressing squegging, as shown in Figure 4(c). Since removal of squegging reduces the input

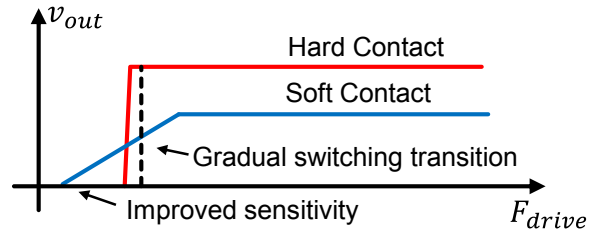


Figure 5: Gain characteristics of hard and soft-contact. Hard contact has instantaneous on/off switching behavior while soft-contact has gradual gain. Soft-contact achieves a lower ultimate voltage and smaller onset switching input due to suppressed squegging.

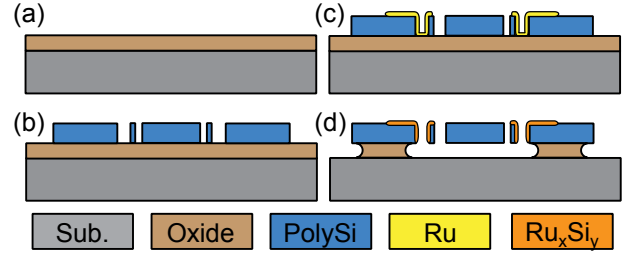


Figure 6: Resoswitch fabrication process.

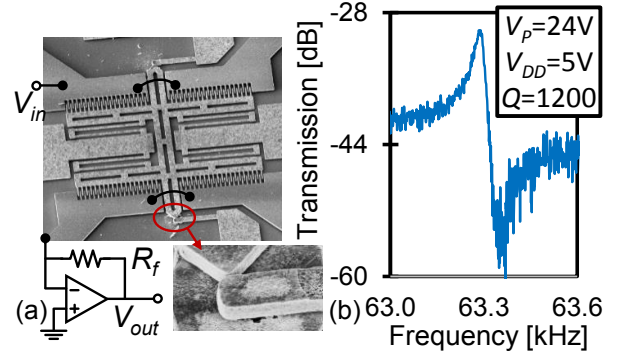


Figure 7: (a) SEM of fabricated poly-silicon resoswitch with Ru-silicided switch tip. (b) Measured transmission spectrum of the resoswitch.

energy needed to impact on every cycle, use of a soft contact electrode also improves the sensitivity at maximum bit rate, as shown in Figure 5, which plots gain characteristics for hard and soft contacts.

## FABRICATION

Figure 6 presents the two-mask fabrication process that achieved soft-contact resoswitches. The process starts with deposition of  $2\mu\text{m}$  LPCVD oxide on a Si substrate, followed by  $2\mu\text{m}$  LPCVD polysilicon, which is subsequently patterned to define the resoswitch structure.  $150\text{nm}$  of Ru is then sputtered and patterned by lift-off to leave metal only over  $10\mu\text{m}$  by  $10\mu\text{m}$  areas at the contact points. The sample is slightly tilted at about  $15^\circ$  during sputtering to ensure metal coverage on the sidewalls of the contact areas. A rapid-thermal-anneal (RTA) at  $950^\circ\text{C}$  for 3 minutes then forms  $\text{Ru}_x\text{Si}_y$  wherever metal touches silicon, while metal over oxide remains intact. A wet dip in Ru etchant removes the unsilicided metal. The silicidation step preferentially leaves silicide over the contact surfaces, but not on the rest of the structure, allowing for higher  $Q$  than if the entire structure were silicided. Finally, a timed etch in 49% HF releases the suspended structure while retaining

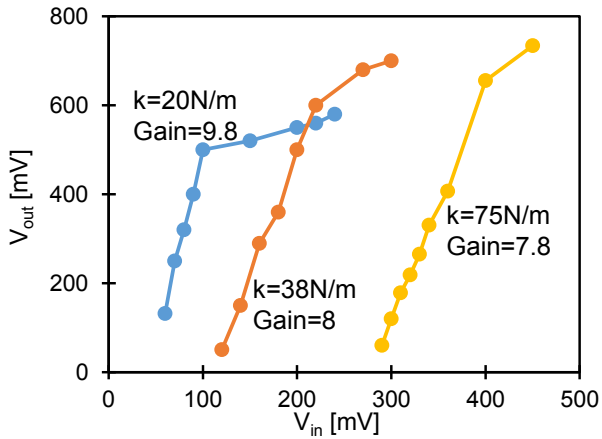


Figure 8: Voltage transfer characteristics delineating the gain of the resoswitch versus soft-impact electrode stiffness.

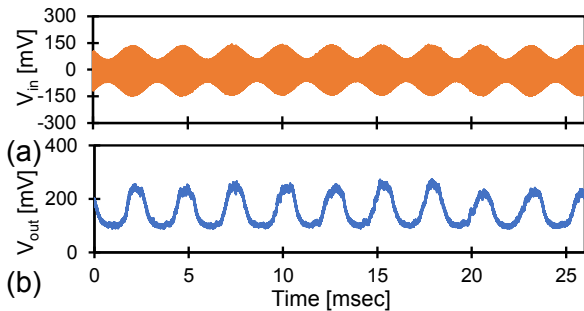


Figure 9: (a) Input AM waveform applied to a soft-impact resoswitch and (b) measured demodulated output.

oxide under anchor areas. Figure 7(a) presents the SEM of a released structure with a zoom-in on the silicide contact.

## EXPERIMENTAL RESULTS

Fabricated devices were measured via probing in a Lakeshore FWPX vacuum probe station under 1mTorr pressure. A Tektronix AFG3200 signal generator provided the AM modulated input, while an oscilloscope monitored the receiver output.

Figure 7(b) presents the frequency response of the polysilicon resoswitch with silicide contact measured in vacuum using the circuit in Figure 7(a) with  $R_f = 100\text{k}\Omega$ . As shown, the measured  $Q$  is only 1200, which is 4 times higher than a previous all-metal resoswitch [1], but lower than the tens of thousands normally expected from a polysilicon resonator. One possible cause for this is galvanic reaction between metal and polysilicon during the HF release step that erodes the polysilicon material, attacking grain boundaries and compromising its structural integrity. Although an improved process is desirable, this process again at least improves over previous ones [1].

Figure 8 plots output voltage (or stored charge across  $C_L$ ) versus input voltage amplitude for three different cantilever stiffness values, with effective gains taken from the slopes. The softer cantilever has the highest gain of 9.8 as well as the highest sensitivity around 60mV, which converts to  $-68\text{dBm}$  when accounting for the mismatch between the  $50\Omega$  signal source and the resoswitch's  $11\text{M}\Omega$  motional impedance. That the softer cantilever provides the highest gain is consistent with FEA's prediction that contact time decreases with decreasing cantilever stiffness.

Once emplaced into the circuit of Figure 2 with  $V_P=25\text{V}$  and  $V_{DD}=5\text{V}$ , the resoswitch becomes a receiver. Since  $V_P$  merely charges the input electrode-to-resoswitch capacitive gap, no current flows, so no power is consumed. Upon reception of an out-of-channel input, the resoswitch shuttle does not move, there is no impact, no current drawn from  $V_{DD}$ , so still, the receiver consumes no power, even though it is on and listening. In other words, it consumes zero quiescent power. Only when a valid input in the desired channel is detected does impacting occur, drawing current from  $V_{DD}$ , and thereby finally consuming power to follow the envelope of the input waveform, as described earlier.

Figure 9 presents the output waveform response in (b) to a 63-kHz carrier AM input signal shown in (a), clearly demonstrating this device's ability to first select the desired carrier while rejecting out-of-channel interferers, then envelope detect to yield the desired de-modulated waveform.

## CONCLUSION

By successfully demodulating 63-kHz AM signal powers as low as  $-68\text{dBm}$  while consuming zero quiescent power, the demonstrated soft-impact resoswitch receiver aligns to the current WWVB wireless time transfer standard and might soon find use in other ultra-low power wireless synchronizing and updating applications. It further encourages use in higher data-rate constellations, such as the more complex QAM (Quadrature AM). The power savings of this technology is particularly compelling for sensor networks whose sensor nodes must listen for incoming commands at all times, especially those for which sensor placements prohibit battery replacement.

**Acknowledgment:** This work was supported by DARPA's N-ZERO program.

## REFERENCES

- [1] R. Liu, J. Naghsh Nilchi, *et al.*, "Zero Quiescent Power VLF ..." in *Transducers*, Anchorage, 2015.
- [2] J. Lowe, "Enhanced WWVB ..." in *Time and Frequency Services*, NIST, 2012.
- [3] J. Brank, *et al.*, "RF MEMS-based ..." *Int J RF  $\mu$ wave Comp Aid Eng*, vol. 11, no. 5, pp. 276-284, 2001.
- [4] R. Nathanael, *et al.*, "4-terminal ..." in *IEDM*, 2009.
- [5] W. Tang, T.-C. H. Nguyen, *et al.*, "Electro-static comb drive ..." *Sensors and Actuators*, Vols. A21-23, pp. 328-331, 1990.
- [6] S. Majumder, N. McGruer, *et al.*, "Study of contacts ..." *Sensors and Actuators A: Physical*, vol. 93, no. 1, pp. 19-26, 2001.
- [7] S. Shaw and P. Holmes, "A periodically forced ..." *Journal of Sound and Vibration*, vol. 90, no. 1, pp. 129-155, 1983.
- [8] K. Shivakumar, W. Elber and W. Illg, "Prediction of impact force and duration ..." *Transactions of ASME*, vol. 52, pp. 674-680, 1985.
- [9] Y. Lin, R. Liu, *et al.*, "Polycide contact interface ..." in *MEMS*, San Francisco, 2014.

## CONTACT

\*R. Liu, liur@eecs.berkeley.edu